

Apparent Dimensionality Dependence of Glassy Dynamics – Infinite Growth of Acoustic Vibrations in Two Dimensions

Hayato Shiba,^{1,2,*} Yasunori Yamada,^{2,†} Takeshi Kawasaki,³ and Kang Kim^{4,5}

¹*Institute for Solid State Physics, University of Tokyo, Chiba 277-8581, Japan*

²*Institute for Materials Research, Tohoku University, Sendai 980-8577, Japan*

³*Department of Physics, Nagoya University, Nagoya 464-8602, Japan*

⁴*Department of Physics, Niigata University, Niigata 950-2181, Japan*

⁵*Division of Chemical Engineering, Graduate School of Engineering Science, Osaka University, Osaka 560-8531, Japan*

(Dated: July 15, 2016)

By using large-scale molecular dynamics simulations, the dynamics of two-dimensional (2D) supercooled liquids turns out to be dependent on the system size, while the size dependence is not pronounced in three dimensional (3D) systems. It is demonstrated that the strong system size effect in 2D amorphous systems originates from the enhanced fluctuations at long wavelengths, which are similar to those of 2D crystal phonons. This observation is further supported by the frequency dependence of the vibrational density of states, consisting of the Debye approximation in the low-wavenumber limit. However, the system size effect in the intermediate scattering function becomes negligible when the length scale is larger than the vibrational amplitude. This suggests that the finite-size effect in a 2D system is transient and also that the structural relaxation itself is not fundamentally different from that in a 3D system. In fact, the dynamic correlation lengths estimated from the bond-breakage function, which do not suffer from those enhanced fluctuations, are not size dependent both in 2D and 3D systems.

PACS numbers: 64.70.kj, 66.30.hh, 61.20.Lc, 46.40.-Bf

Dimensionality plays a key role in the physics of solids and liquids – from high to low dimensions, and fluctuation shows up differently, as typically observed in phase transitions [1, 2]. Indeed, two-dimensional (2D) systems often exhibit enhanced fluctuations, leading to various anomalies that are not experienced in three-dimensional (3D) systems. The melting of a 2D solid is a marked example [3–9], where the long-wavelength structural correlation is induced by thermal fluctuations stemming over an infinite length. For the glass transition from supercooled liquids to amorphous solids, the dimensionality dependence of the fluctuation has become the issue only recently. Gigantic fluctuation in 2D supercooled liquids has been observed that is far stronger than that in their 3D counterparts [10–12]. The aim of this Letter is to elucidate the similarity of this fluctuation to that in crystals, and also to investigate the heterogeneous dynamics both in 2D and 3D systems.

For a crystalline solid of monodisperse particles assemblies, the variance in the thermal displacement is given by using the vibrational density of state (VDOS) $g(\omega)$ as a function of angular frequency ω as

$$\langle |u|^2 \rangle = \frac{dk_B T}{m} \int \frac{g(\omega)}{\omega^2} d\omega, \quad (1)$$

where m the particle mass, d the spatial dimension, and $(k_B T)^{-1}$ the inverse temperature. This is related to the vibration amplitude A_p by $2\langle |u|^2 \rangle = A_p^2$. Under the Debye approximation for the density of acoustic plane waves, $g(\omega)$ becomes proportional to ω^{d-1} [13]. It leads to divergence of the integral in 2D systems owing to the low-frequency acoustic waves, while it converges in 3D systems. As a result, the long-ranged translation order is prohibited in 2D systems [14, 15]. Such divergence of the vibration amplitude in 2D systems can be

restarted as a function of the linear system length L , by integrating Eq. (1) over $\omega > 2\pi/(L/c)$ as

$$\langle |u|^2 \rangle \sim \frac{k_B T}{2\pi} \left(\frac{1}{\mu} + \frac{1}{K + \mu} \right) \ln \left(\frac{L}{\sigma_0} \right), \quad (2)$$

where μ and K are shear and bulk moduli, σ_0 is the particle radius, and c is the velocity of sound. Such fluctuation is the source of the size dependent behavior of 2D solids undergoing melting [4, 6, 7, 9].

In amorphous solids, $g(\omega)$ is known to behave quite differently from that in crystals. Simulations [16–21] and experiments [22–26] indicate abundance of acoustic excitations in amorphous solids, exhibiting the so-called “boson peak”. For the frequencies far lower than the boson peak, the Debye model can be supposed because the microscopic details are irrelevant to long-wavelength modes [24, 27]. Several attempts have been made to verify the Debye model description on the microscopic basis by using molecular simulations [19, 28], but no conclusive simulation data have been provided on the asymptotic behaviors at low frequencies. Therefore, it is still an open issue how these low-frequency vibration modes affect the dimensionality dependence of thermal fluctuations.

In this study, we address the dimensionality dependence of the low-frequency thermal vibrations and the dynamics. The 2D binary 50:50 soft-sphere (2D SS) supercooled liquid [29] and the 3D binary 80:20 Kob–Andersen Lennard–Jones (3D KALJ) [30] are used. The pair potential of 2D SS is given by $v_{\alpha\beta}(r) = \epsilon_{\alpha\beta}(\sigma_{\alpha\beta}/r)^{12}$ for $r < r_c = 2.21\sigma_1$, where the cubic smoothing function $v_{\alpha\beta}(r) = B(a - r)^3 + C$ for distances $r > r_c$, with the values of a , B , and C satisfying continuity condition at $r = r_c$. The size and mass ratios are $\sigma_2/\sigma_1 = 1.4$ and $m_2/m_1 = 1.96$, and $\epsilon_{\alpha\beta} = 1$ for all the pairs. For the 3D KALJ, the pair potential is given by

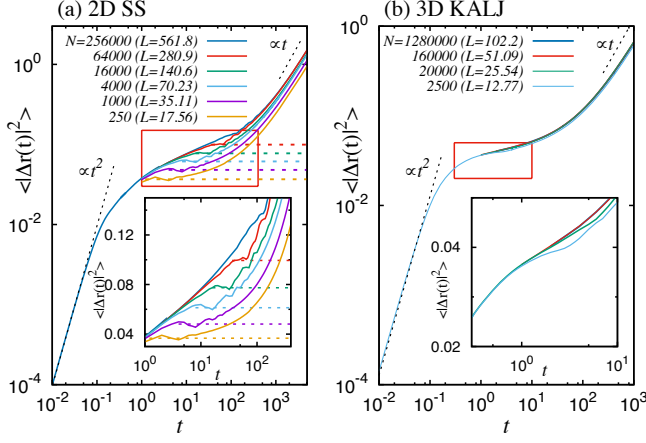


FIG. 1. Size dependence of the MSD $\langle |\Delta \mathbf{r}(t)|^2 \rangle$ of (a) 2D SS at $T = 0.64$ and (b) 3D KALJ at $T = 0.47$ for various system sizes. In the insets, the respective plateau regions (indicated by the red box) are magnified. In (a), the height of the plateaus are indicated by the dotted lines.

$v_{\alpha\beta}(r) = 4\epsilon_{\alpha\beta}[(\sigma_{\alpha\beta}/r)^{12} - (\sigma_{\alpha\beta}/r)^6]$, in which $\alpha, \beta \in \{1, 2\}$, with the detailed settings are the same as those in Ref. 31, except for the particle number. The number densities $n = N/L^d$ in 2D SS for $T=0.64$. Red filled circles represent half the plateau height in Fig. 1 (a), red solid line stands for the direct integration of Eq. (1) in the range $2\pi/(L/c_T) < \omega < \infty$ in (a), and black dotted line is the estimate by Eq. (2). (d) The VDOS $g(\omega)$ obtained from the VCF of 3D KALJ for $N = 10240000$. Black dotted line represents the estimation by the Debye approximation. Inset: The VDOS obtained with $N = 160000$ over the whole ω .

is $\tau = \sqrt{m_1 \sigma_1^2 / \epsilon_{11}}$,

First, we study the means-square displacements (MSD) $\langle |\Delta \mathbf{r}(t)|^2 \rangle = \langle (1/N) \sum_j [\mathbf{r}_j(t) - \mathbf{r}_j(0)]^2 \rangle$ of 2D SS and 3D KALJ. Between the short-time ballistic and long-time diffusive regimes, a plateau due to the thermal vibration emerges, and its height represents the mean-squared vibrational amplitude $A_p^2 = 2\langle |\mathbf{u}|^2 \rangle$ [10] as a result of superpositions of vibrations over a range of frequencies. In Fig. 1, the MSDs $\langle |\Delta \mathbf{r}(t)|^2 \rangle$ are plotted for (a) 2D SS and (b) 3D KALJ. For $N = 250, 1000, 4000$, and 16000 in 2D SS, the plateaus are distinctly observed, as indicated by the dotted lines. The plateau is a bit raised for $N = 64000$, exhibiting a crossover to the long-time diffusive regime. Finally, the plateau disappears for $N = 256000$. In 3D KALJ in (b), on the other hand, the MSDs exhibit virtually no size dependence for $N \geq 2500$.

These size dependence is attributed to the long-wavelength acoustic sound modes, represented in the VDOS at low frequencies comparable to $\omega \sim 2\pi/(L/c)^{-1}$ – the limiting behavior in the limit of $\omega \rightarrow 0$ matters. Although the VDOS is usually estimated by the normal mode analysis, it becomes more difficult as the system size becomes larger, because the eigenvector calculation of the N^2 Hessian matrix is required. As an alternative, the VDOS is obtained by directly calculating the velocity correlation function (VCF) as

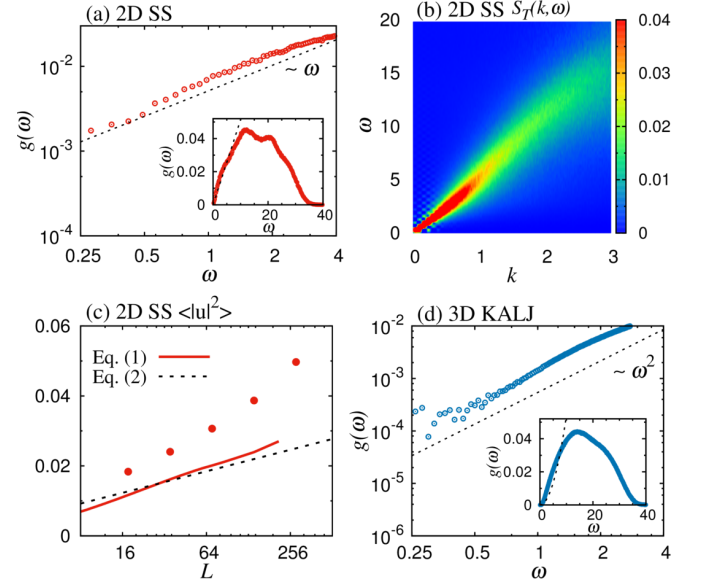


FIG. 2. (a) The VDOS $g(\omega)$ of 2D SS for $N = 256000$. The black dotted line represents the VDOS estimated by the Debye approximation. Inset: The same VDOS over the whole ω . (b) Color plot of the DSF for the transverse wave $S_T(k, \omega)$ of 2D SS, representing the linear dispersion relationship. (c) Displacement variance $\langle |\mathbf{u}|^2 \rangle = A_p^2/2$ in 2D SS for $T=0.64$. Red filled circles represent half the plateau height in Fig. 1 (a), red solid line stands for the direct integration of Eq. (1) in the range $2\pi/(L/c_T) < \omega < \infty$ in (a), and black dotted line is the estimate by Eq. (2). (d) The VDOS $g(\omega)$ obtained from the VCF of 3D KALJ for $N = 10240000$. Black dotted line represents the estimation by the Debye approximation. Inset: The VDOS obtained with $N = 160000$ over the whole ω .

$g(\omega) = 2(\pi d N k_B T)^{-1} \int dt e^{i\omega t} \sum_j \langle m_j \mathbf{v}_j(0) \cdot \mathbf{v}_j(t) \rangle$ [18], The time development of the thermal vibration has been simulated at low temperatures, $T = 0.01$ for 2D SS and 0.008 for 3D KALJ. The initial particle configuration is prepared by the steepest descent method, in order to begin the simulation from the local potential minimum. We find that these temperatures are low enough that the obtained VDOS provides the faithful description of the normal modes. In Fig. 2 (a), the VDOS is shown for 2D SS at $N = 256000$. In the limiting behavior $\omega \rightarrow 0$, the VDOS clearly exhibits linear ω -dependence. In the Debye theory of the crystalline solids [13], the VDOS can be explicitly estimated to be $g_D(\omega) = \omega/(2\pi n c_M^2)$, where $c_M^{-2} = (c_L^{-2} + c_T^{-2})/2$, with c_L and c_T being the longitudinal and transverse sound velocities, respectively. The VDOS asymptotically approaches $g_D(\omega)$, assuming up to 1.4 times larger values in the present frequency region. The sound velocities are estimated by dynamic structure factors (DSFs) $S_{L,T}(k, \omega) = 2\bar{m}(d\pi N k_B T)^{-1} \int dt e^{i\omega t} \langle \mathbf{j}_{L,T}(\mathbf{k}, 0) \cdot \mathbf{j}_{L,T}(\mathbf{k}, t) \rangle$ with $\mathbf{j}_{L,T}(\mathbf{k}, t)$ the longitudinal and transverse current velocity [21, 32] and \bar{m} the average particle mass. The wavenumbers $k = |\mathbf{k}|$ at the peak values of the DSFs satisfy the linear dispersion relations $\omega = c_{L,T}k$, as seen for $S_T(k, \omega)$ of 2D SS in Fig. 2 (b). The linear fit provides the estimate values of sound velocities as $c_L = 8.6$ and 11.9 and $c_T = 3.8$ and 4.7 for

2D SS and 3D KALJ, respectively.

The 2D plateau height in the MSD (specifically, its half value $A_p^2/2$) in Fig. 1 (a) can be compared with the mean-squared variance $\langle |\mathbf{u}|^2 \rangle$ calculated by using Eq. (2) and also with the direct integration of Eq. (1) with the mass m replaced by the average \bar{m} . From the linear dispersion relation, the shear and bulk moduli of 2D SS in Eq. (2) are estimated to be $\mu = \rho c_T^2 = 26.6$ and $K = \rho c_L^2 - \mu = 142.1$, respectively, with $\rho = \bar{m}n$ being the mass density. For both Eqs. (1) and (2), the low-frequency integration is simply cut off at $\omega_{\text{min}} = 2\pi c_T/L$, which provides only an approximation that should not strictly hold on the quantitative level. In Fig. 2 (c), these quantities are plotted as a function of L . Both Eqs. (1) and (2) provide lower values than the estimation from the plateau height, but exhibit similar divergence with L . Therefore, the Debye-like behavior is the source of the system size dependence of the amplitude in 2D systems. For the direct integration of $g(\omega)$ in Fig. 2 (a), the size dependence is mainly due to a small number of available low-frequency modes ($\omega \lesssim \tau^{-1}$). On that account, the integration is performed for $L < 211\sigma_1$.

Also, in 3D systems, the VDOS is expected to exhibit Debye-type behavior at low-frequencies. This is shown for 3D KALJ with $N = 10240000$ in Fig. 2 (d), and is also shown over the whole range of ω for $N = 160000$ in its inset. In the low-frequency region, the VDOS exhibits $g(\omega) \sim \omega^{d-1}$ dependence. The VDOS asymptotically approaches the VDOS $g_D(\omega) = \omega^2/(2\pi^2 n c_M^3)$ in the Debye approximation, where $c_M^{-3} = (c_L^{-3} + 2c_T^{-3})/3$. The low-frequency modes have small influences on the integration of Eq. (1) because $g(\omega) \sim \omega^2$ rapidly goes to zero in the $\omega \rightarrow 0$ limit. This fact consists with the lack of finite size effects in $\langle |\mathbf{u}|^2 \rangle$ in 3D KALJ. The VDOS still exhibits the values from 2 to 2.6 times larger values in the present frequency region, in qualitative consistency with the previous experimental observation where VDOS is few times larger than the Debye description [24]. It remains an open question whether the VDOS further approaches Debye-type behavior at lower frequencies or not.

Now that the source of the 2D anomaly has been revealed, we address the resultant dimensionality dependence of the relaxation times, dynamic susceptibility, and the dynamic correlation lengths in the reminder of this Letter. To begin with, the system-size dependence of the self-part of the intermediate scattering function $F_s(k, t) = (1/N) \sum_j \exp[i\mathbf{k} \cdot (\mathbf{r}_j(t) - \mathbf{r}_j(0))]$ is shown for 2D SS in Fig. 3. In addition to the standard choice of the wavenumber $k = 2\pi/\sigma_1$, the smaller three wavenumbers ($k = 2\pi/\lambda$, with $\lambda = 2\sigma_1, 4\sigma_1$, and $8\sigma_1$) are adopted. $F_s(k, t)$ relaxes faster with larger system sizes for $\lambda = \sigma_1$, in consistency with a previous result for 2D KALJ [11]. For larger λ , the relaxation is observed to be independent of the system size. Therefore, the particle motion on a length scale a few times larger than σ_1 does not depend on the system size, while motion on the particle-size scale depends (note that A_p amounts to about $0.3\sigma_1$ in Fig. 2 (c)). The finite-size effect is observed just as a transient effect taking place at short time and length scales induced by vibrations. It is backed by the periodic transient peaks due to the sound waves traversing over

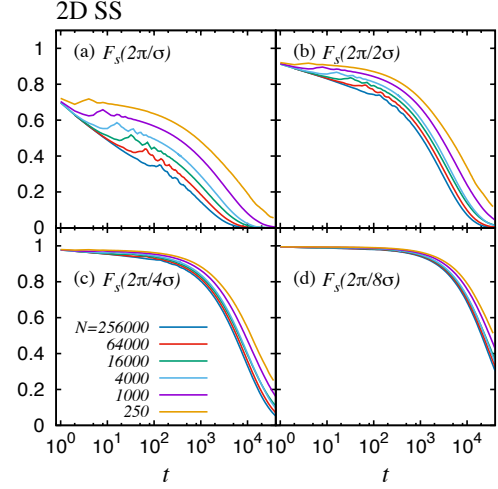


FIG. 3. Size dependence of $F_s(k = 2\pi/\lambda, t)$ of 2D SS at $T = 0.64$ is plotted, for $\lambda =$ (a) σ_1 , (b) $2\sigma_1$, (c) $4\sigma_1$, and (d) $8\sigma_1$.

the system for small values of λ . In 3D systems, $F_s(k, t)$ (not shown) is independent of the system size, even for $\lambda = \sigma_1$.

In light of the above discussions, we now discuss the resulting difference in the characteristic times and dynamic correlation lengths between 2D and 3D systems. The difference can be discussed in terms of the four-point function [10, 33–35] and bond-breakage correlation function [10, 36–38]. The four-point function characterizes the configuration overlap between different times by using the overlap function $W_i(a, t) = \Theta(a - |\mathbf{r}_i(t) - \mathbf{r}_i(0)|)$, where $\Theta(x)$ is the Heaviside step function and a the overlap threshold distance. The spatiotemporally heterogeneous dynamics can be probed through its dynamic susceptibility $\chi_4(t) = N[\langle W(t)^2 \rangle - \langle W(t) \rangle^2]$, where $W(t) = (1/N) \sum_j W_j(a, t)$ and the four-point structure factor $S_4(k, t) = (1/N) \langle \sum_{m,n} W_m(t) W_n(t) \exp[i\mathbf{k} \cdot (\mathbf{r}_m(0) - \mathbf{r}_n(0))] \rangle$, with j, m , and n being the particle indices. a is set to $0.3\sigma_1$, which is a length comparable to the vibration amplitude A_p for the 2D system. The results are summarized in Fig. 4. As shown in Fig. 4 (a), $\chi_4(t)$ exhibits sharp peaks for large system sizes $N \geq 64000$ at $t = (n + \frac{1}{2}) \frac{L}{c_T}$ ($n = 0, 1, 2, \dots$) (open arrows) owing to the transverse sound waves traversing the whole periodic system. Although the transient peaks encompass the whole time regimes, we conjecture that t_4 should be the overall peak (filled arrows) that can still be estimated for $N \leq 64000$. $S_4(k, t)$ is estimated at the peak time t_4 of $\chi_4(t)$ that maximizes the heterogeneity of the configuration overlap. The other variable, broken-bond number $Z_j(t)$, addresses the correlation time and length caused by the change in the local particle connectivity [10, 37, 39]. More specifically, $Z_j(t)$ is the number of particles j neighboring i at time t_0 ($r_{ij} < A_1\sigma_{\alpha\beta}$) getting separated at a later time $t_0 + t$ ($r_{ij} > A_2\sigma_{\alpha\beta}$), with $A_2 > A_1$. The threshold distances are set as $(A_1, A_2) = (1.2, 1.5)$ for 2D SS and $(1.3, 1.65)$ for 3D KALJ. $Z_j(t)$ starts from 0 at the initial time $t = 0$ and increases one by one as t proceeds, as a pair of bonded particles get separated from each other.

The bond-breakage function treats pure rearrangement motion caused by the particle jumps[40, 41], and excludes the effect of collective motion, which the overlap function involves. A difference can arise when vibrations over large particle clusters take place with large amplitudes. The bond-breakage susceptibility and structure factors can then be defined by $\chi_B(t) = N[\langle Z(t)^2 \rangle - \langle Z(t) \rangle^2]$ where $Z(t) = (1/N) \sum_j Z_j(t)$ and $S_B(k, t) = (1/N) \langle \sum_{m,n} Z_m(t) Z_n(t) \exp[i\mathbf{k} \cdot (\mathbf{r}_n(0) - \mathbf{r}_m(0))] \rangle$. $S_B(k, t)$ is estimated at the peak time t_B of $\chi_B(t)$ that turns out to be several times larger than t_4 . From both $S_4(k, t_4)$ and $S_B(k, t_B)$, the respective dynamic correlation lengths ξ_4 and ξ_B can be estimated by fitting with the generalized Ornstein–Zernike (OZ) function [31]. Figure 4 (b) shows both of the structure factors for 2D SS as functions of wavenumber k . While $S_4(k, t_4)$ exhibits strong divergence with N at small k , $S_B(k, t_B)$ exhibits no size dependence. For 2D SS, Figs. 4 (c) and (d) show that the α -relaxation time τ_α , and four-point time and length t_4 and ξ_4 exhibit strong size dependence owing to the vibration motion. This is attributed to the size-dependent gigantic vibration amplitude A_p comparable to a . In contrast, t_B and ξ_B exhibit no size dependence. This is attributed to the correlation length of the slow and heterogeneous dynamics owing to particle rearrangement after elimination of the vibrational effect. The overlap function fails to correctly characterize the rearrangement dynamics. For the glassy relaxation itself, there is no system-size dependence even in 2D systems.

For 3D KALJ, t_4 and t_B exhibit no size dependence for $N \geq 2500$. The structure factors $S_4(k, t_4)$ and $S_B(k, t_B)$ in Fig. 4 (e) show that there are no finite size effects in the dynamics. For all the range of temperatures under investigation, the two dynamic correlation lengths ξ_4 and ξ_B exhibit a perfect coincidence, as shown in Fig. 4 (f). Therefore, it is clear that low-frequency vibrations do not influence the relaxation time and the dynamic length in 3D KALJ.

In this Letter, we have shown the existence of strong vibrational fluctuations in 2D systems whose amplitude grows to the limit of $N \rightarrow \infty$, and its influence on the dynamic correlation time and lengths. Our observations establish that long-ranged fluctuations arise due to a similar mechanism to that in 2D crystalline solids. In the low-frequency regime, ω^{d-1} asymptotic behavior is similar to the prediction of the Debye approximation, but the value is still larger, *i.e.*, low-frequency plane waves are more abundant than in the crystal both for 2D and 3D systems. In 2D systems, the self-correlation function of the density and the four-point function fail to characterize the slow structural correlation, and the original structural glassy relaxation can be characterized by observing the shorter time scale motion. Indeed, the broken-bond correlation function is trivially free from the transient dynamics induced by the long-wavelength vibration motion. This is the reason why the system size dependence vanishes, and its correlation length ξ_B is expected to assume the true dynamic correlation length. Therefore, there are two different dynamic effects in the 2D supercooled liquid, *i.e.*, particle jump motions and long-wavelength acoustic sound modes. The former consists of the glassy relaxation itself, and heterogeneous dy-

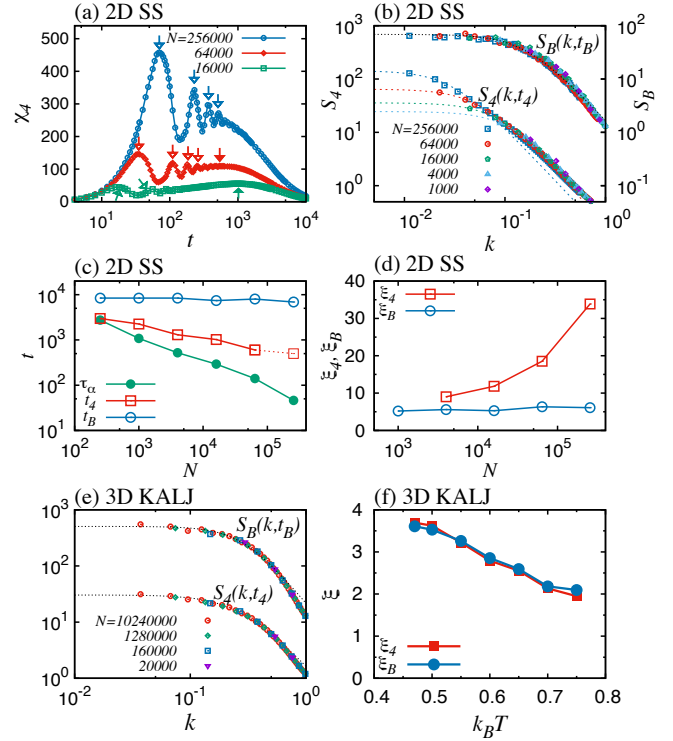


FIG. 4. (a) and (b) show the size dependence of $\chi_B(t)$ and $S_4(k, t_4)$ of 2D SS at $T = 0.64$, respectively. Open arrows in (a) indicate the peaks originating in the transverse sound modes, and filled arrows ($N \leq 64000$) shows t_4 . Dotted lines in (b) represent the generalized OZ fit for each. (c) and (d) show the relaxation and correlation times (τ_α , t_4 , t_B) and the correlation lengths (ξ_4 , ξ_B) of 2D SS, with t_4 of $N = 256000$ conjectured by the extrapolation. (e) Size dependence of $S_4(k, t_4)$ and $S_B(k, t_B)$ of 3D KALJ at $T = 0.47$. Dotted lines represent the generalized OZ fits for $N = 10240000$. (f) Temperature dependence of ξ_4 and ξ_B are plotted for 3D KALJ with $N = 1280000$.

namics is proven to exhibit no size dependence. The mechanism of the original glassy relaxation is shown to be the similar between the 2D and 3D systems, apart from the transient vibrational dynamics.

We thank Akira Onuki for motivating us to perform this work. We also thank Kunimasa Miyazaki, Ryoichi Yamamoto, Atsushi Ikeda, and Hideyuki Mizuno for helpful discussions. This work was partially supported by JSPS KAKENHI Grant Numbers JP25103010 (HS), JP15H06263 and JP16H06018 (TK), and JP26400428 and JP16H00829 (KK). HS and YY were also financially supported by Building of Consortia for the Development of Human Resources in Science and Technology, MEXT, Japan. The numerical calculations were carried out on SGI Altix ICE 8400EX and XA at ISSP, University of Tokyo and on Fujitsu PRIMERGY RX300 S7 at RCCS, NINS, Okazaki, Japan.

* E-mail: shiba@imr.tohoku.ac.jp

[†] Present Address: Beijing Computational Science Research Center, Beijing 100193, China

- [1] N. D. Mermin and H. Wagner, Phys. Rev. Lett. **17**, 1133 (1966).
- [2] J. M. Kosterlitz and D. J. Thouless, J. Phys. C Solid State Phys. **6**, 1181 (1973).
- [3] B. I. Halperin and D. R. Nelson, Phys. Rev. Lett. **41**, 121 (1978).
- [4] H. Weber, D. Marx, and K. Binder, Phys. Rev. B **51**, 14636 (1995).
- [5] K. J. Strandburg, Rev. Mod. Phys. **60**, 161 (1988).
- [6] H. Shiba, A. Onuki, and T. Araki, EPL **86**, 66004 (2009).
- [7] E. P. Bernard and W. Krauth, Phys. Rev. Lett. **107**, 155704 (2011).
- [8] S. Deuschländer, A. M. Puertas, G. Maret, and P. Keim, Phys. Rev. Lett. **113**, 127801 (2014).
- [9] M. Mazars, EPL **110**, 26003 (2015).
- [10] H. Shiba, T. Kawasaki, and A. Onuki, Phys. Rev. E **86**, 041504 (2012).
- [11] E. Flenner and G. Szamel, Nat. Commun. **6**, 7392 (2015).
- [12] S. Vivek, C. P. Kelleher, P. M. Chaikin, and E. R. Weeks, (2016), arXiv:1604.07338.
- [13] N. W. Ashcroft and N. D. Mermin, *Solid State Physics* (Thomson Learning, Toronto, 1976).
- [14] B. Jancovici, Phys. Rev. Lett. **19**, 20 (1967).
- [15] Y. Imry and L. Gunther, Phys. Rev. B **3**, 3939 (1971).
- [16] W. Schirmacher, G. Diezemann, and C. Ganter, Phys. Rev. Lett. **81**, 136 (1998).
- [17] N. Xu, M. Wyart, A. J. Liu, and S. R. Nagel, Phys. Rev. Lett. **98**, 175502 (2007).
- [18] H. Shintani and H. Tanaka, Nat. Mater. **7**, 870 (2008).
- [19] G. Monaco and S. Mossa, Proc. Natl. Acad. Sci. U. S. A. **106**, 16907 (2009).
- [20] P. Tan, N. Xu, A. B. Schofield, and L. Xu, Phys. Rev. Lett. **108**, 095501 (2012).
- [21] A. Marruzzo, W. Schirmacher, A. Fratalocchi, and G. Ruocco, Sci. Rep. **3**, 1407 (2013).
- [22] E. Duval, A. Boukenter, and T. Achibat, J. Phys. Condens. Matter **2**, 10227 (1990).
- [23] G. N. Greaves and S. Sen, Adv. Phys. **56**, 1 (2007).
- [24] G. Monaco and V. M. Giordano, Proc. Natl. Acad. Sci. U. S. A. **106**, 3659 (2009).
- [25] K. Chen, W. G. Ellenbroek, Z. Zhang, D. T. N. Chen, P. J. Yunker, S. Henkes, C. Brito, O. Dauchot, W. van Saarloos, A. J. Liu, and A. G. Yodh, Phys. Rev. Lett. **105**, 025501 (2010).
- [26] A. I. Chumakov, G. Monaco, A. Monaco, W. A. Crichton, A. Bosak, R. Rüffer, A. Meyer, F. Kargl, L. Comez, D. Fioretto, H. Giefers, S. Roitsch, G. Wortmann, M. H. Manghnani, A. Hushur, Q. Williams, J. Balogh, K. Parliński, P. Jochym, and P. Piekarczyk, Phys. Rev. Lett. **106**, 225501 (2011).
- [27] C. L. Klix, G. Maret, and P. Keim, Phys. Rev. X **5**, 041033 (2015).
- [28] F. Leonforte, R. Boissière, A. Tanguy, J. P. Wittmer, and J. L. Barrat, Phys. Rev. B **72**, 224206 (2005).
- [29] R. Yamamoto and A. Onuki, J. Phys. Soc. Jpn. **66**, 2545 (1997).
- [30] W. Kob, C. Donati, S. J. Plimpton, P. H. Poole, and S. C. Glotzer, Phys. Rev. Lett. **79**, 2827 (1997).
- [31] K. Kim and S. Saito, J. Chem. Phys. **138**, 12A506 (2013).
- [32] H. Mizuno, S. Mossa, and J.-L. Barrat, Proc. Natl. Acad. Sci. U. S. A. **111**, 11949 (2014).
- [33] N. Lačević, F. W. Starr, T. B. Schroder, and S. C. Glotzer, J. Chem. Phys. **119**, 7372 (2003).
- [34] G. Szamel and E. Flenner, Phys. Rev. E **74**, 021507 (2006).
- [35] E. Flenner, M. Zhang, and G. Szamel, Phys. Rev. E **83**, 051501 (2011).
- [36] R. Yamamoto and A. Onuki, Phys. Rev. E **58**, 3515 (1998).
- [37] T. Kawasaki and A. Onuki, Phys. Rev. E **87**, 012312 (2013).
- [38] E. Flenner and G. Szamel, J. Stat. Mech. **2016**, 074008 (2016).
- [39] T. Iwashita, D. M. Nicholson, and T. Egami, Phys. Rev. Lett. **110**, 205504 (2013).
- [40] R. Pastore, A. Coniglio, and M. Pica Ciamarra, Soft Matter **10**, 5724 (2014).
- [41] R. Pastore, A. Coniglio, A. de Candia, A. Fierro, and M. P. Ciamarra, J. Stat. Mech. **2016**, 054050 (2016).